Atmos. Chem. Phys. Discuss., 14, 29101–29157, 2014
www.atmos-chem-phys-discuss.net/14/29101/2014/
doi:10.5194/acpd-14-29101-2014

Atmospheric Chemistry and Physics Discussions
Open Access

First and second derivative atmospheric CO_2, global surface temperature and ENSO

L. M. W. Leggett and D. A. Ball

Global Risk Policy Group Pty Ltd, Townsville, Queensland, Australia

Received: 3 May 2014 – Accepted: 19 October 2014 – Published: 21 November 2014

Correspondence to: L. M. W. Leggett (mleggett.globalriskprogress@gmail.com)

Published by Copernicus Publications on behalf of the European Geosciences Union.

Abstract

A significant gap now of some 16 years in length has been shown to exist between the observed global surface temperature trend and that expected from the majority of climate simulations, and this gap is presently continuing to increase. For its own sake, and to enable better climate prediction for policy use, the reasons behind this mismatch need to be better understood. While an increasing number of possible causes have been proposed, the candidate causes have not yet converged.

The standard model which is now displaying the disparity has it that temperature will rise roughly linearly with atmospheric CO_2. However research also exists showing correlation between the interannual variability in the growth rate of atmospheric CO_2 and temperature. Rate of change of CO_2 had not been a causative mechanism for temperature because it was concluded that causality ran from temperature to rate of change of CO_2.

However more recent studies have found little or no evidence for temperature leading rate of change of CO_2 but instead evidence for simultaneity. With this background, this paper reinvestigated the relationship between rate of change of CO_2 and two of the major climate variables, atmospheric temperature and the El Niño–Southern Oscillation (ENSO).

Using time series analysis in the form of dynamic regression modelling with autocorrelation correction, it is demonstrated that first-derivative CO_2 leads temperature and that there is a highly statistically significant correlation between first-derivative CO_2 and temperature. Further, a correlation is found for second-derivative CO_2, with the Southern Oscillation Index, the atmospheric-pressure component of ENSO. This paper also demonstrates that both these correlations display Granger causality.

It is shown that the first-derivative CO_2 and climate model shows no trend mismatch in recent years.

These results may contribute to the prediction of future trends for global temperature and ENSO.

ACPD

14, 29101–29157, 2014

Granger causality from the 1st/2nd derivatives of atmospheric CO_2

L. M. W. Leggett and D. A. Ball

Interannual variability in the growth rate of atmospheric CO_2 is standardly attributed to variability in the carbon sink capacity of the terrestrial biosphere. The terrestrial biosphere carbon sink is created by photosynthesis: a major way of measuring global terrestrial photosynthesis is by means of satellite measurements of vegetation reflectance, such as the Normalized Difference Vegetation Index (NDVI). This study finds a close correlation between an increasing NDVI and the increasing climate model/temperature mismatch (as quantified by the difference between the trend in the level of CO_2 and the trend in temperature).

1 Introduction

Understanding current global climate requires an understanding of trends both in Earth's atmospheric temperature and the El Niño–Southern Oscillation (ENSO), a characteristic large-scale distribution of warm water in the tropical Pacific Ocean and the dominant global mode of year-to-year climate variability (Holbrook et al., 2009). However, despite much effort, the average projection of current climate models has become statistically significantly different from the 21st century global surface temperature trend (Fyfe et al., 2013, 2014) and has failed to reflect the statistically significant evidence that annual-mean global temperature has not risen in the twenty-first century (Fyfe, 2013; Kosaka, 2013).

The situation is illustrated visually in Fig. 1 which shows the increasing departure over recent years of the global surface temperature trend from that projected by a representative climate model (the CMIP3, SRESA1B scenario model for global surface temperature, KNMI 2013). It is noted that the level of atmospheric CO_2 is a good proxy for the IPCC models predicting the global surface temperature trend: according to IPCC AR5 (2013), on decadal to interdecadal time scales and under continually increasing effective radiative forcing, the forced component of the global surface temperature trend responds to the forcing trend relatively rapidly and almost linearly.

ACPD
14, 29101–29157, 2014

Modelling also provides a wide range of predictions for future ENSO variability, some showing an increase, others a decrease and some no change (Guilyardi et al., 2012; Bellenger, 2013). The extremes of this ENSO variability cause extreme weather (such as floods and droughts) in many regions of the world.

A wide range of physical explanations has now been proposed for the global warming slowdown. Chen and Tang (2014) place the explanations into two categories. The first involves a reduction in radiative forcing: by a decrease in stratospheric water vapour, an increase in background stratospheric volcanic aerosols, by 17 small volcano eruptions since 1999, increasing coal-burning in China, the indirect effect of time-varying anthropogenic aerosols, a low solar minimum, or a combination of these. The second category of candidate explanation involves planetary sinks for the excess heat. The major focus for the source of this sink has involved ocean heat sequestration. However, evidence for the precise nature of the ocean sinks is not yet converging. According to Chen and Tang (2014) their study followed the original proposal of Meehl et al. (2011) that global deep-ocean heat sequestration is centred on the Pacific. However, their observational results were that such deep-ocean heat sequestration is mainly occurring in the Atlantic and the Southern oceans.

Alongside the foregoing possible physical causes, Hansen et al. (2013) has suggested that the pause in the global temperature increase since 1998 might be caused by the planetary biota, in particular the terrestrial biosphere: that is (IPCC, 2007), the fabric of soils, vegetation and other biological components, the processes that connect them and the carbon, water and energy they store.

It is widely considered that the interannual variability in the growth rate of atmospheric CO_2 is a sign of the operation of the influence of the planetary biota. Again, IPCC (2007) states: "The atmospheric CO_2 growth rate exhibits large interannual variations. The change in fossil fuel emissions and the estimated variability in net CO_2 uptake of the oceans are too small to account for this signal, which must be caused by year-to-year fluctuations in land–atmosphere fluxes." In the IPCC Fourth Assessment Report, Denman et al. (2007) state (italics denote present author emphasis): "Interan-

ACPD
14, 29101–29157, 2014

L. M. W. Leggett and D. A. Ball

nual and inter-decadal variability in the growth rate of atmospheric CO_2 is dominated by the *response of the land biosphere to climate variations*. ... The terrestrial biosphere *interacts strongly with the climate*, providing both positive and negative feedbacks due to biogeophysical and biogeochemical processes. ... Surface climate is determined by the balance of fluxes, which can be changed by radiative (e.g., albedo) or non-radiative (e.g., water cycle related processes) terms. Both radiative and non-radiative terms *are controlled by details of vegetation*."

Denman et al. (2007) also note that many studies have confirmed that the variability of CO_2 fluxes is mostly due to land fluxes, and that tropical lands contribute strongly to this signal. A predominantly terrestrial origin of the growth rate variability can be inferred from (1) atmospheric inversions assimilating time series of CO_2 concentrations from different stations (2) consistent relationships between $\delta^{13}C$ and CO_2 (3) ocean model simulations and (4) terrestrial carbon cycle and coupled model simulations. For one prominent estimate carried out by the Global Carbon Project, the land sink is calculated as the residual of the sum of all sources minus the sum of the atmosphere and ocean sinks (Le Quere et al., 2014).

The activity of the land sink can also be estimated directly. The terrestrial biosphere carbon sink is created by photosynthesis: a major way of measuring global land photosynthesis is by means of satellite measurements of potential photosynthesis from greenness estimates. The predominantly used such measure is the Normalized Difference Vegetation Index (NDVI) (Running et al., 2004; Zhang et al., 2014). NDVI data are available from the start of satellite observations in 1980 to the present. For this period the trend signature in NDVI has been shown to correlate closely with that for atmospheric CO_2 (Barichivich et al., 2013). This noted, we have not been able to find studies which have compared NDVI data with the difference between climate models and temperature.

ACPD
14, 29101–29157, 2014

2 Methodological issues and objectives of the study

2.1 Methodological issues

Before considering further material it is helpful now to consider a range of methodological issues and concepts. The first concept is to do with the notion of causality.

According to Hidalgo and Sekhon (2011) there are four prerequisites to enable an assertion of causality. The first is that the cause must be prior to the effect. The second prerequisite is "constant conjunction" (Hume, 1751, cited in Hidalgo and Sekhon, 2011) between variables. This relates to the degree of fit between variables. The final requirements are those concerning manipulation; and random placement into experimental and control categories. It is noted that each of the four prerequisites is necessary but not sufficient for causality.

Concerning the last two criteria, the problem for global studies such as global climate studies is that manipulation and random placement into experimental and control categories cannot be carried out.

One method using correlational data, however, approaches more closely the quality of information derived from random placement into experimental and control categories. The concept is that of Granger causality (Granger, 1969). According to Stern and Kaufmann (2014) a time series variable "x" (e.g. atmospheric CO_2) is said to "Granger-cause" variable "y" (e.g. surface temperature) if past values of x help predict the current level of y, better than do just the past values of y, given all other relevant information.

Reference to the above four aspects of causality will be made to help structure the review of materials in the following sections.

2.2 Objectives of the study

What has been considered to influence the biota's creation of the pattern observed in the trend in the growth rate of atmospheric CO_2? The candidates for the influences on

Discussion Paper | Discussion Paper | Discussion Paper | Discussion Paper |

ACPD

14, 29101–29157, 2014

Granger causality from the 1st/2nd derivatives of atmospheric CO_2

L. M. W. Leggett and D. A. Ball

the biota have mainly been considered in prior research to be atmospheric variations, primarily temperature and/or ENSO (e.g., Kuo et al., 1990; W. Wang et al., 2013). Despite its proposed role in global warming overall, CO_2 (in terms of the initial state of atmospheric CO_2 exploited by plants at time A) has not generally been isolated and studied in detail through time series analysis as an influence in the way the biosphere influences the CO_2 left in the atmosphere at succeeding time B.

This state of affairs seems to have come about for two reasons, one concerning ENSO, the other, temperature. For ENSO, the reason is that the statistical studies are unambiguous that ENSO leads rate of change of CO_2 (for example, Lean and Rind, 2008). On the face of it, therefore, this ruled out CO_2 as the first mover of the ecosystem processes. For temperature, the reason was that the question of whether atmospheric temperature leads rate of change of CO_2 or vice versa is less settled.

In the first published study on this question, Kuo et al. (1990) provided evidence that the signature of interannual atmospheric CO_2 (measured as its first derivative) fitted temperature (passing therefore one of the four tests for causality, of close conjunction).

The relative fits of both level of and first derivative of atmospheric CO_2 with global surface temperature up to the present are depicted in Fig. 2. Attention is drawn to both signature (fine grained data structure) and, by means of polynomial smoothing, core trend for each data series.

Concerning signature, while clearly first-derivative CO_2 and temperature are not identical, each is more alike than either is to the temperature model based on level of CO_2. As well, the polynomial fits show that the same likeness groupings exist for core trend.

Kuo et al. (1990) also provided evidence concerning another of the causality prerequisites – priority. This was that the signature of first-derivative CO_2 *lagged* temperature (by 5 months). This idea has been influential. More recently, despite Adams and Piovesan (2005) noting that climate variations, acting on ecosystems, are believed to be responsible for variation in CO_2 increment, but there are major uncertainties in identifying processes (including uncertainty concerning) *instantaneous* (present authors' em-

ACPD
14, 29101–29157, 2014

phasis) vs. lagged responses; and W. Wang et al. (2013) observing that the strongest coupling is found between the CO_2 growth rate and the *concurrent* (present authors' emphasis) tropical land temperature, C. Wang et al. (2013) nonetheless state in their conclusion that the strong temperature–CO_2 coupling they observed is best explained by the additive responses of tropical terrestrial respiration and primary production to temperature variations, which reinforce each other in enhancing *temperature's control* (present author emphasis) on tropical net ecosystem exchange.

Another perspective on the relative effects of rising atmospheric CO_2 concentrations on the one hand and temperature on the other has been provided by extensive direct experimentation on plants. In a large scale meta-analysis of such experiments, Dieleman et al. (2012) drew together results on how ecosystem productivity and soil processes responded to combined warming and CO_2 manipulation, and compared it with those obtained from single factor CO_2 and temperature manipulation. While the meta-analysis found that responses to combined CO_2 and temperature treatment showed the greatest effect, this was only slightly larger than for the CO_2-only treatment. By contrast the effect of the CO_2-only treatment was markedly larger than for the warming-only treatment.

Concerning leading and lagging climate series more generally, the first finding of correlations between the rate of change (in the form of the first derivative) of atmospheric CO_2 and a climate variable was with the foregoing and the Southern Oscillation Index (SOI) component of ENSO (Bacastow, 1976). Here evidence was presented that the SOI led first-derivative atmospheric CO_2. There have been further such studies (see Imbers, 2013 for overview) which, taken together, consistently show that the highest correlations are achieved with SOI leading temperature, by some months (3–4 months).

In light of the foregoing this paper reanalyses by means of time series regression analysis the question of which of first-derivative CO_2 and temperature leads which, The joint temporal relationship between interannual atmospheric CO_2, global surface temperature and ENSO (indicated by the SOI) is also investigated.

ACPD
14, 29101–29157, 2014

The foregoing also shows that a strong case can be made for further investigating the planetary biota influenced by atmospheric CO_2 as a candidate influence on (cause of) climate outcomes. This question is also explored in this paper.

A number of Granger causality studies have been carried out on climate time series (see review in Attanasio, 2012). Of papers we have found which assessed atmospheric CO_2 and global surface temperature – some six (Sun and Wang, 1996; Triacca, 2005; Kodra et al., 2011; Attanasio and Triacca, 2011; Attanasio, 2012; Stern and Kaufmann, 2014) – while all but one (Triacca, 2005) found Granger causality, it was not with CO_2 concentration but with CO_2 radiative forcing ($\ln CO_2$, Attanasio and Triacca, 2011).

As well, all studies used annual not monthly data. Such annual data for each of atmospheric CO_2 and temperature is not stationary of itself but must be made stationary by differencing (Sun and Wang, 1996). Further, data at this level of aggregation can "mask" correlational effects that only become apparent when higher frequency (e.g., monthly) data are used.

To our knowledge the question of stationarity and other time series questions concerning the relationship between atmospheric CO_2 and temperature have not been attempted using CO_2 concentration rather than CO_2 radiative forcing and monthly rather than annual data.

Short of Granger causality analysis, another method of assessment used has been multiple linear regression, either corrected or uncorrected for autocorrelation. This method has frequently been used to quantify the relative importance of natural and anthropogenic influencing factors on climate outcomes such as global surface temperature – for example, Lean and Rind (2008, 2009); Foster and Rahmstorf (2011); Kopp and Lean (2011); Zhou and Tung (2013). It is noted that while multiple regression analysis can at best *assume* a causal direction between the variables being modelled, Granger causality analysis provides a formal testing of this assumption (Granger, 1969).

From such studies, a common set of main influencing factors (also called explanatory or predictor variables) has emerged. These are (Lockwood, 2008; Folland, 2013;

Zhou and Tung, 2013): El Nino–Southern Oscillation (ENSO), or Southern Oscillation alone (SOI); volcano aerosol optical depth; total solar irradiance; and the anthropogenic warming trend. In these models, ENSO/SOI is the factor embodying interannual variation. Imbers et al. (2013) show that a range of different studies using these variables have all produced similar and close fits with the global surface temperature.

With this background this paper first presents an analysis concerning whether the first derivative of atmospheric CO_2 leads or lags global surface temperature. That assessed, questions of autocorrelation, strength of correlation, and of causality are then explored. Given this exploration of correlations involving first-derivative atmospheric CO_2, the possibility of the correlation of second difference CO_2 with climate variables is also explored.

Correlations are assessed at a range of time scales to seek the time extent over which relationships are held, and thus whether they are a special case or possibly longer term in nature. The time scales involved are, using instrumental data, over two periods starting respectively from 1959 and 1877; and, using paleoclimate data, over a period commencing from 1515. The correlations are assessed by means of regression models explicitly incorporating autocorrelation using dynamic regression modelling methods. Granger causality between CO_2 and, respectively, temperature and SOI is also explored. Atmospheric CO_2 rather than emissions data is used, and where possible at monthly rather than annual aggregation. Finally, as noted, we have not been able to find studies which have compared the gap between climate models and temperature with NDVI data so an assessment of this question is carried out. All assessments were carried out using the time series statistical software packages Gnu Regression, Econometrics and Time-series Library (GRETL) and IHS Eviews.

3 Data and methods

We present results of time series analyses of climate data. The data assessed are global surface temperature, atmospheric carbon dioxide (CO_2) and the Southern Os-

ACPD
14, 29101–29157, 2014

cillation Index (SOI). The regressions are presented in several batches based on the length of data series for which the highest temporal resolution is available. The first batch of studies involves the data series for which the available high resolution series is shortest: this is for atmospheric carbon dioxide (CO_2) and commences in 1958. These studies are set at monthly resolution.

The second batch of studies is for data able to be set at monthly resolution not involving CO_2. These studies begin with the time point at which the earliest available monthly SOI data commences, 1877.

The final batch of analyses utilises annual data. These studies use data starting variously in the 16th or 18th centuries.

Data from 1877 and more recently is from instrumental sources; earlier data is from paleoclimate sources.

For instrumental data sources for global surface temperature we used the Hadley Centre–Climate Research Unit combined land SAT and SST (HadCRUT) version 4.2.0.0 (Morice et al., 2012), for atmospheric CO_2 the US Department of Commerce National Oceanic & Atmospheric Administration Earth System Research Laboratory Global Monitoring Division Mauna Loa, Hawaii monthly CO_2 series (Keeling et al., 2009), and for volcanic aerosols the National Aeronautic and Space Administration Goddard Institute for Space Studies Stratospheric Aerosol Optical Thickness series (Sato et al., 1993). Southern Oscillation Index (SOI) data (Troup,1965) is from from the Science Delivery Division of the Department of Science, Information Technology, Innovation and the Arts (DSITIA) Queensland Australia. Solar irradiance data is from Lean (J. Lean, personal communication, 2012).

The Southern Oscillation is the atmospheric-pressure component of ENSO, and is an oscillation in the surface air pressure between the tropical eastern and the western Pacific Ocean waters. It is calculated from normalized Tahiti minus Darwin sea level pressure. In contrast, the El Niño component of ENSO is specified in terms of changes in the Pacific Ocean sea surface temperature relative to the average temperature. In this study it is considered to be simpler to conduct an analysis in which the temperature

ACPD
14, 29101–29157, 2014

is an outcome (dependent variable) without also having (Pacific Ocean) temperature as an input (independent variable). The correlation between SOI and the other ENSO indices is high, so we believe this assumption is robust.

Paleoclimate data sources are: atmospheric CO_2, from 1500: ice cores (Robertson et al., 2001); (NH) temperature, from 1527: tree ring data (Moberg et al., 2005); SOI: from 1706: tree ring data (Stahle et al., 1998).

Normalized Difference Vegetation Index (NDVI) monthly data from 1980 to 2006 is from the GIMMS (Global Inventory Modeling and Mapping Studies) data set, accessed via KNMI (2014). NDVI data from 2006 to 2013 was provided by the Institute of Surveying, Remote Sensing and Land Information, University of Natural Resources and Life Sciences, Vienna.

Statistical methods used are standard (Greene, 2012). Categories of methods used are: normalisation; differentiation (approximated by differencing); and time series analysis. Within time series analysis, methods used are: smoothing; leading or lagging of data series relative to one another to achieve best fit; assessing a prerequisite for using data series in time series analysis, that of stationarity; including autocorrelation in models by use of dynamic regression models; and investigating causality by means of a multivariate time series model, known as a vector autoregression (VAR) and its associated Granger causality test. These methods will now be described in turn.

To make it easier to visually assess the relationship between the key climate variables, the data were normalised using statistical Z scores or standardised deviation scores (expressed as "Relative level" in the figures). In a Z scored data series, each data point is part of an overall data series that sums to a zero mean and variance of 1, enabling comparison of data having different native units. See the individual figure legends for details on the series lengths.

In the time series analysis SOI and global atmospheric surface temperature are the dependent variables. For these two variables, we tested the relationship between (1) the change in atmospheric CO_2 and (2) the variability in its rate of change. We express these CO_2-related variables as finite differences, which is a convenient approximation

ACPD
14, 29101–29157, 2014

to derivatives (Hazewinkel, 2001; Kaufmann et al., 2006). The finite differences used here are of both the first- and second-order types (we label these "first" and "second" differences in the text). Variability is explored using both intra-annual (monthly) data and interannual (yearly) data. The period covered in the figures is shorter than that used in the data preparation because of the loss of some data points due to calculations of differences and of moving averages (in monthly terms of up to 13 × 13), which commenced in January 1960.

Smoothing methods are used to the degree needed to produce similar amounts of smoothing for each data series in any given comparison. Notably, to achieve this outcome, series resulting from higher levels of differences require more smoothing. Smoothing is carried out initially by means of a 13 month moving average – this also minimises any remaining seasonal effects. If further smoothing is required, then this is achieved (Hyndman, 2010) by taking a second moving average of the initial moving average (to produce a double moving average). Often, this is performed by means of a further 13 month moving average to produce a 13 × 13 moving average. For descriptive statistics to describe the long-term variation of a time series trend, polynomial smoothing is sometimes used.

Variables are led or lagged relative to one another to achieve best fit. These leads or lags were determined by means of time-lagged correlations (correlograms). The correlograms were calculated by shifting the series back and forth relative to each other, 1 month at a time.

With this background, the convention used in this paper for unambiguously labelling data series and their treatment after smoothing or leading or lagging is depicted in the following example. The atmospheric CO_2 series is transformed into its second derivative and smoothed twice with a 13 month moving average. The resultant series is then *Z* scored. This is expressed as Z2x13mma2ndDerivCO_2.

As well, it is noted that, to assist readability in text involving repeated references, atmospheric CO_2 is sometimes referred to simply as CO_2 and global surface temperature as temperature.

ACPD
14, 29101–29157, 2014

The time series analysis methodology used in this paper involves the following procedures. First, any two or more time series being assessed by time series regression analysis must be what is termed stationary in the first instance, or be capable of being made stationary (by differencing). A series is stationary if its properties (mean, variance, covariances) do not change with time (Greene, 2012). Dickey–Fuller stationarity tests are calculated for each variable.

Second, the residuals from any time series regression analysis then conducted must not be significantly different from white noise. This is done seeking correct model specification for the analysis.

After Greene (2012), the results of standard ordinary least squares (OLS) regression analysis assume that the errors in the model are uncorrelated. Autocorrelation of the errors violates this assumption. This means that the OLS estimators are no longer the Best Linear Unbiased Estimators (BLUE). Notably and importantly this does not bias the OLS coefficient estimates. However statistical significance can be overestimated, and possibly greatly so, when the autocorrelations of the errors at low lags are positive.

Addressing autocorrelation can take either of two alternative forms: *correcting for it* (for example, for first order autocorrelation by the Cochrane–Orcutt procedure), or *taking it into account*.

In the latter approach, the autocorrelation is taken to be a consequence of an inadequate specification of the temporal dynamics of the relationship being estimated. The method of dynamic regression modelling (Pankratz, 1991) addresses this by seeking to explain the current behavior of the dependent variable in terms of both contemporaneous and past values of variables. In this paper the dynamic modelling approach is taken.

To assess the extent of autocorrelation in the residuals of the initial non-dynamic OLS models run, the Breusch–Godfrey procedure is used. Dynamic models are then used to take account of such autocorrelation. To assess the extent to which the dynamic models achieve this, Kiviet's Lagrange multiplier F test (LMF) statistic for autocorrelation (Kiviet, 1986) is used.

ACPD
14, 29101–29157, 2014

Hypotheses related to Granger causality (see Sect. 1) are tested by estimating a multivariate time series model, known as a vector autoregression (VAR), for level of, and first-derivative CO_2 and other relevant variables. The VAR models the current values of each variable as a linear function of their own past values and those of the other variables. Then we test the hypothesis that x does not cause y by evaluating restrictions that exclude the past values of x from the equation for y and vice versa.

Stern and Kander (2011) observe that Granger causality is not identical to causation in the classical philosophical sense, but it does demonstrate the likelihood of such causation (or the lack of such causation) more forcefully than does simple contemporaneous correlation. However, where a third variable, z, drives both x and y, x might still appear to drive y though there is no actual causal mechanism directly linking the variables (any such third variable must have some plausibility – see Sect. 5 below).

4 Results

4.1 Relationship between first-derivative CO_2 and temperature

4.1.1 Priority

Figure 2 showed that while clearly first-derivative CO_2 and temperature are not identical in signature, each is more alike than either is to the temperature model based on level of CO_2. As well the figure shows that the same likeness relationships exist for the core trend. The purpose of the forthcoming sections is to see the extent to which these impressions are statistically significant.

The first question assessed is that of priority: which of first-derivative atmospheric CO_2 and global surface temperature leads the other. The two series are shown for the period 1959 to 2012 in Fig. 3.

It is not possible to discern from the above plot which precise relative phasing of the two series leads to the best fit and hence the answer to the question of which series

ACPD
14, 29101–29157, 2014

leads which. To quantify the degree of difference in phasing between the variables, time-lagged correlations (correlograms) were calculated by shifting the series back and forth relative to each other, one month at a time.

First, what does the above relationship look like in correlogram form, and what is the appearance of the correlograms for the other commonly used global temperature categories – tropical, Northern Hemisphere and Southern Hemisphere? These correlograms are given in Fig. 4.

It can be seen that, for all four relationships shown, first-derivative CO_2 always leads temperature. The leads differ as quantified in Table 1.

It is possible for a lead to exist overall on average but for a lag to occur for one or other specific subsets of the data. This question is explored in Fig. 5 and Table 2. Here the full 1959–2012 period of monthly data – some 640 months – for each of the temperature categories is divided into three approximately equal sub-periods, to provide 12 correlograms. It can be seen that in all 12 cases, first-derivative CO_2 leads temperature. It is also noted that earlier sub-periods tend to display longer first-derivative CO_2 leads. For the most recent sub-period the highest correlation is when the series are neither led nor lagged.

4.1.2 Correspondence between first-derivative CO_2 and global surface temperature curves

Next, the second prerequisite for causality, close correspondence, is also seen between first-derivative CO_2 and global surface temperature in Fig. 3.

4.1.3 Time series analysis

The robustness of both first-derivative CO_2 leading temperature and the two series displaying close correspondence is a firm basis for the time series analysis to follow of the statistical relationship between first-derivative CO_2 and temperature. For this further analysis we choose global surface temperature as the temperature series because,

ACPD
14, 29101–29157, 2014

while its maximum correlation is not the highest (Fig. 5), its global coverage by definition is greatest.

The following sections provide the results of the time series analysis. (In this section, TEMP stands for global surface temperature (Hadcrut4), and other block capital terms are those used in the modelling.) First, as stated above, all series used in a time series regression must be stationary (Greene, 2012). By means of the Augmented Dickey–Fuller (ADF) test for stationarity Table 3 provides the information concerning stationarity for level of and first-derivative CO_2 and global surface temperature.

The table shows that, for the monthly series used, the variables TEMP and FIRST-DERIVATIVE CO_2 are both stationary.

In contrast, the variable CO_2 is non-stationary (specifically, it is integrated of order one, i.e., I(1)). Here an important result arises: attempting to assess TEMP in terms of the level of CO_2 would result in an "unbalanced regression", as the dependent variable (TEMP) and the explanatory variable (CO_2) have different orders of integration. It is well known (e.g., Banerjee et al., 1993, p. 190–191, and the references therein) that in unbalanced regressions the t-statistics are biased away from zero. That is, one can appear to find statistically significant results when in fact they are not present. In fact, that occurs when we regress TEMP on CO_2. This reason alone is strong evidence that any analysis should involve the variables TEMP and FIRST-DERIVATIVE CO_2, and not TEMP and CO_2.

Nonetheless one can explore the extent to which first-derivative CO_2 and climate variable correlations are statistically significant and so might make first-derivative CO_2 a candidate in its own right as a cause of climate trends.

For the variables for which stationarity is established, one must next assess the extent if any of autocorrelation affecting the time series model. This is done by obtaining diagnostic statistics from an OLS regression. This regression shows, by means of the Breusch–Godfrey test for autocorrelation (up to order 12 – that is, including all monthly lags up to 12 months), that there is statistically significant autocorrelation

ACPD
14, 29101–29157, 2014

at lags of one and two months, leading to an overall Breusch–Godfrey Test statistic (LMF) = 126.901238, with p value = $P(F(12\,626) > 126.901) = 1.06 \times 10^{-158}$.

The autocorrelation is taken to be a consequence of an inadequate specification of the temporal dynamics of the relationship being estimated. With this in mind, a dynamic model (Greene, 2012) with two lagged values of the dependent variable as additional independent variables has been estimated. Full results are shown in Supplementary Table S1. There, the LMF test shows that there is now no statistically significant unaccounted-for autocorrelation, thus supporting the use of this dynamic model specification.

Inspection of Table S1 shows that a highly statistically significant model has been established. First it shows that the temperature in a given period is strongly influenced by the temperature of closely preceding periods. (See Discussion for a possible mechanism for this.) Further it provides evidence that there is also a clear, highly statistically significant role in the model for first-derivative CO_2.

4.1.4 Granger causality analysis

We now can turn to assessing if first-derivative atmospheric CO_2 may not only correlate with, but also contribute causatively to, global surface temperature. This is done by means of Granger causality analysis.

Recalling that both TEMP and FIRST-DERIVATIVE CO_2 are stationary, it is appropriate to test the null hypothesis of no Granger causality from FIRST-DERIVATIVE CO_2 to TEMP by using a standard Vector Autoregressive (VAR) model without any transformations to the data. The Akaike Information Criterion (AIC) and the Schwartz Information Criterion (SIC) were used to select an optimal maximum lag length (k) for the variables in the VAR. This lag length was then lengthened, if necessary, to ensure that:

i. The estimated model was dynamically stable (i.e., all of the inverted roots of the characteristic equation lie inside the unit circle);

ii. The errors of the equations were serially independent.

ACPD
14, 29101–29157, 2014

The relevant EViews output from the VAR model is entitled VAR Granger Causality/Block Exogeneity Wald Tests and documents the following summary results: Wald Statistic (p value): null is there is No Granger Causality from first-derivative CO_2 to TEMP Number of lags $K = 4$; Chi-Square 26.684 (p value = 0.000).

A p value of this level is highly statistically significant and means the null hypothesis of No Granger Causality is very strongly rejected. That is, over the period studied there is strong evidence that first-derivative CO_2 Granger-causes TEMP.

Despite the lack of stationarity in the level of CO_2 time series meaning it cannot be used to model temperature, one can still assess the answer to the question: "Is there evidence of Granger causality between level of CO_2 and TEMP?"

In answering this question, because the TEMP series is stationary, but the CO_2 series is non-stationary (it is integrated of order one), the testing procedure is modified slightly. Once again, the levels of both series are used. For each VAR model, the maximum lag length (k) is determined, but then one additional lagged value of both TEMP and CO_2 is included in each equation of the VAR. However, the Wald test for Granger non-causality is applied only to the coefficients of the original k lags of CO_2. Toda and Yamamoto (1995) show that this modified Wald test statistic will still have an asymptotic distribution that is chi-square, even though the level of CO_2 is non-stationary.

Here the relevant Wald Statistic (p value): null is there is No Granger Causality from level of CO_2 to TEMP Number of lags $K = 4$; Chi-Square 2.531 (p value = 0.470).

The lack of statistical significance in the p value is strong evidence that level of CO_2 does not Granger-cause TEMP.

With the above two assessments done, it is significant that concerning global surface temperature we are able to discount causality involving the level of CO_2, but establish causality involving first-derivative CO_2.

ACPD
14, 29101–29157, 2014

4.2 Relationship between second-derivative CO_2 and temperature and Southern Oscillation Index

4.2.1 Priority and correspondence

Given the results of this exploration of correlations involving first-derivative atmospheric CO_2, the possibility of the correlation of second-derivative CO_2 with climate variables is also explored. The climate variables assessed are global surface temperature and the Southern Oscillation Index (SOI). In this section, data is from the full period for which monthly instrumental CO_2 data is available, 1958 to the present. For this period, the series neither led nor lagged appear as follows (Fig. 6):

Let us look (Fig. 6) at the two key pairs of interannually varying factors. For the purpose of this figure, to facilitate depiction of trajectory, second-derivative CO_2 and SOI (right axis) are offset so that all four curves display a similar origin in 1960.

The figure shows that, alongside the already demonstrated close similarity between first-derivative CO_2 and temperature, there is a second apparent distinctive pairing between second-derivative CO_2 and SOI.

The figure shows that the overall trend, amplitude and phase – the signature – of each pair of curves is both matched within each pair and different from the other pair. The remarkable sorting of the four curves into two groups is readily apparent. Each pair of results provides context for the other – and highlights the different nature of the other pair of results.

Recalling that even uncorrected for any autocorrelation, correlational data still holds information concerning regression coefficients, we initially use OLS correlations without assessing autocorrelation to provide descriptive statistics. Table 4 includes, first without any phase shifting to seek to maximise fit, the full six pairwise correlations arising from all possible combinations of the four variables other than with themselves. Here it can be seen that the two highest correlation coefficients (in bold in the table) are, first, between first-derivative CO_2 and temperature, and, second, between second-derivative CO_2 and SOI.

ACPD
14, 29101–29157, 2014

In Table 5 phase shifting has been carried out to maximise fit (shifts shown in variable titles in the table). This results in an even higher correlation coefficient for second-derivative CO_2 and SOI.

The link between all three variable realms – CO_2, SOI and temperature – can be further observed in Fig. 7 and Table 6. Figure 7 shows SOI, second-derivative atmospheric CO_2 and first-derivative temperature, each of the latter two series phase-shifted for maximum correlation with SOI (as in Table 5). Concerning priority, Table 6 shows that maximum correlation occurs when second-difference CO_2 leads SOI. It is also noted that the correlation coefficients for the correlations between the curves shown in Table 6 have all converged in value compared to those shown in Table 5.

Concerning differences between the curves shown in Fig. 7, two of what major departures there are between the curves are coincide with volcanic aerosols – from the El Chichon volcanic eruption in 1982 and the Pinatubo eruption in 1992 (Lean and Rind, 2009). These factors taken into account, it is notable when expressed in the form of the transformations in Fig. 7 that the signatures of all three curves are so essentially similar that it is almost as if all three curves are different versions of – or responses to – the same initial signal.

So, a case can be made that first and second-derivative CO_2 and temperature and SOI respectively are all different aspects of the same process.

4.2.2 Time series analysis

Let us more formally assess the relationship between second-derivative CO_2 and SOI. As for first-derivative CO_2 and temperature above, stationarity has been established. Again, similarly to first-derivative CO_2 and temperature, there is statistically significant autocorrelation at lags of one and two months, leading to an overall Breusch–Godfrey Test statistic (LMF) of 126.9, with p value = $P(F(12\,626) > 126.901) = 1.06 \times 10^{-158}$.

Table S2 shows the results of a dynamic model with the dependent variable used at each of the two lags as further independent variables.

ACPD
14, 29101–29157, 2014

In Table S2 the results first show (LMF test) that there is now no statistically significant unaccounted-for autocorrelation.

Further inspection of Table S2 shows that a highly statistically significant model has been established. As for temperature, it shows that the SOI in a given period is strongly influenced by the SOI of closely preceding periods. Again as for temperature it provides evidence that there is a clear role in the model for second-derivative CO_2.

With this established, it is noted that while the length of series in the foregoing analysis was limited by the start date of the atmospheric CO_2 series (January 1958), high temporal resolution (monthly) SOI goes back considerably further, to 1877. This long period SOI series (for background see Troup, 1965) is that provided by the Australian Bureau of Meteorology, sourced here from the Science Delivery Division of the Department of Science, Information Technology, Innovation and the Arts, Queensland, Australia. As equivalent temperature data is also available (the global surface temperature series already used above (HADCRUT4) goes back as far as 1850), these two longer series are now plotted in Fig. 8.

What is immediately noted is the continuation over this longer period of the striking similarity between the two signatures already shown in Fig. 7.

Turning to regression analysis, as previously the Breusch–Godfrey procedure shows that, for lags up to lag 12, the lion's share of autocorrelation is again restricted to the first two lags. Table S3 shows the results of a dynamic model with the dependent variable used at each of the two lags as further independent variables.

In comparison with Table S2, the extended time series modelled in Table 9 shows a remarkably similar R-squared statistic: 0.466 compared with 0.477. By contrast, the partial regression coefficient for second-derivative CO_2 has increased, to 0.14 compared with 0.077. These points made, the main finding is that there is little or no difference in the relationship when it is extended back to 1877. (It is beyond the scope of this study, but the relationship of SOI and second-derivative CO_2 means it is now possible to produce a proxy for monthly atmospheric CO_2 from 1877: a date approximately 75 years prior to the start in January 1958 of the CO_2 monthly instrumental record.)

ACPD
14, 29101–29157, 2014

4.2.3 Granger causality analysis

This section assesses whether second-derivative CO_2 can be considered to Granger-cause SOI. This assessment is carried out using 1959 to 2012 data.

Test results on the stationarity or otherwise of each series are given in Table 7. Each series is shown to be stationary. These results imply that we can approach the issue of possible Granger causality by using a conventional VAR model, in the levels of the data, with no need to use a "modified" Wald test (as used in the Toda and Yamamoto (1995) methodology).

Simple OLS regressions of SOI against separate lagged values of DCO_2 (including an intercept) confirm the finding that the highest correlation is when a two-period lag is used.

A 2-equation VAR model is needed for reverse-sign SOI and second-derivative CO_2. The first task is to determine the optimal maximum lag length to be used for the variables. Using the SIC, this is found to be 2 lags. When the VAR model is estimated with this lag structure however, Table 8, testing the null hypothesis that there is no serial correlation at lag order h, shows that there is evidence of autocorrelation in the residuals.

This suggests that the maximum lag length for the variables needs to be increased. The best results (in terms of lack of autocorrelation) were found when the maximum lag length is 3. (Beyond this value, the autocorrelation results deteriorated substantially, but the conclusions below, regarding Granger causality, were not altered.)

Table 9 shows that the preferred, 3-lag model, still suffers a little from autocorrelation.

However, as we have a relatively large sample size, this will not impact adversely on the Wald test for Granger causality.

The relevant EViews output from the VAR model is entitled VAR Granger Causality/Block Exogeneity Wald Tests and documents the following summary results: Wald Statistic (p value): null is there is No Granger Causality from second-derivative CO_2 to sign-reversed SOI Chi-Square 22.554 (p value = 0.0001).

ACPD
14, 29101–29157, 2014

The forgoing Wald statistic shows that the null hypothesis is strongly rejected: in other words, there is very strong evidence of Granger Causality from second-derivative CO_2 to sign-reversed SOI.

4.3 Paleoclimate data

So far, the time period considered in this study has been pushed back in the instrumental data realm to 1877. If non-instrumental paleoclimate proxy sources are used, CO_2 data now at annual frequency can be taken further back. The following example uses CO_2 and temperature data. The temperature reconstruction used here commences in 1500 and is that of Frisia et al. (2003), derived from annually laminated speliothem (stalagmite) records. A second temperature record (Moberg et al., 2005) is from tree ring data. The atmospheric CO_2 record (Robertson et al., 2001) is from fossil air trapped in ice cores and from instrumental measurements. The trends for these series are shown in Fig. 9.

Visual inspection of the figure shows that there is a strong overall likeness in signature between the two temperature series, and between them and first-derivative CO_2. The similarity of signature is notably less with level of CO_2. It can be shown that level of CO_2 is not stationary and even with the two other series which are stationary the strongly smoothed nature of the temperature data makes removal of the autocorrelation present impossible. Nonetheless, noting that data uncorrected for autocorrelation still provides valid correlations (Greene, 2012) – only the statistical significance is uncertain – it is simply noted that first-derivative CO_2 displays a better correlation with temperature than level of CO_2, for each temperature series (Table 10).

4.4 Normalized Difference Vegetation Index (NDVI) data

This section now investigates the land biosphere as a candidate for the foregoing effects, in particular the increasing difference between the global surface temperature trend suggested by general circulation climate models and that observed.

ACPD
14, 29101–29157, 2014

The level of atmospheric CO_2 is a good proxy for the IPCC models predicting the global surface temperature trend: according to IPCC AR5 (2013), on decadal to interdecadal time scales and under continually increasing effective radiative forcing (ERF), the forced component of the global surface temperature trend responds to the ERF trend relatively rapidly and almost linearly. On this basis an indicator of the difference between the climate model trend and the observed temperature is prepared by subtracting the Z scored actual temperature trend from the Z scored CO_2 trend.

The trend in the terrestrial CO_2 sink is estimated annually as part of assessment of the well known global carbon budget (Le Quere at al., 2014). It is noted that there is a risk of involving a circular argument concerning correlations between the terrestrial CO_2 sink and interannual (first derivative) CO_2 because the terrestrial CO_2 sink is defined as the residual of the global carbon budget (Le Quere et al., 2014). By contrast, the Normalized Difference Vegetation Index (NDVI) involves direct (satellite-derived) measurement of terrestrial plant activity. For this reason, and because of the two series only NDVI is provided in monthly form, we will use only NDVI in what follows.

Figure 10 plots the trends since the start of the NDVI record in 1981 for the difference between the observed trends in level of atmospheric CO_2 and in global surface temperature; the Southern oscillation index; and global NDVI.

Figure 10 shows the signature of the increasing difference between CO_2 trend and temperature trend in recent years; close apparent correlation of the difference with NDVI; and also with SOI. Perhaps the major variation between the curves coincides with volcanic aerosols from the Pinatubo eruption in 1992 (Lean and Rind, 2009).

The following section assesses the strength of the correlations depicted in Fig. 10. To start with, it is noted that all three series used meet the time-series analysis criterion of stationarity (Dickey–Fuller test, Table 11).

The next two analyses (for full model outputs see Tables S4 and S5) provide dynamic models set up based on Breusch–Godfrey test results indicating the number of lags displaying autocorrelation. The models are for the relationship between the NDVI and, first, the difference between level of CO_2 and temperature, and second, with SOI.

ACPD
14, 29101–29157, 2014

Granger causality from the 1st/2nd derivatives of atmospheric CO_2

L. M. W. Leggett and D. A. Ball

The models show that the partial regression coefficient of NDVI with the difference between level of CO_2 and temperature is statistically significant, and that that with SOI approaches statistical significance.

It is noted from Table S4 and Fig. 10 that the climate variable SOI leads the observed behaviour of the putative causal variable NDVI. Does this remain consistent with the hypothesis put forward in this paper that the first mover in the observed climate cycles might be the detection by plants of the second-derivative CO_2 trend? It is argued that it does remain consistent because, while SOI is shown in Table S5 to lead NDVI, second-derivative CO_2 has earlier (Figs. 7 and 8, and Tables S1 and S2) been shown to lead SOI. (This lead is by two months or three months depending on the period assessed.)

The observation was made above concerning Fig. 7 that the signatures of all three curves in the figure were so essentially similar that it was almost as if all three were different versions of – or responses to – the same initial signal. This set of signatures can now have added to it the further similar signature of the NDVI. It may be that the NDVI embodies the initial signal.

5 Discussion and conclusions

The results from the foregoing are summarised and compared in Table 12.

Table 12 and reference to the relevant figures show that relationships between first and second-derivative CO_2 and climate variables are present at all the time scales studied, that is, including temporal start points situated as long ago as 1500. In the five instances where time series analysis accounting for autocorrelation could be successfully conducted, the results were statistically significant (two tailed test) in four of the five cases, and significant at one-tailed test level in the fifth. While for the two further instances (commencing in 1500) the data was not amenable to time series analysis, the correlations visually observed were consistent with the instances that were. Taken as a whole the results clearly suggest that the mechanism observed is long term, and

ACPD
14, 29101–29157, 2014

not, for example, a creation of the period of steepest anthropogenic CO_2 emissions increase which commenced in the 1950s (IPCC, 2013).

A second notable finding highlighted by the bringing together of results in Table 12 is the major role of immediate past instances of the dependent variable in its own present state. This was found to be the case in all the instances where time series models could be prepared. This was true for both temperature and SOI. This was not to take away from first and second-derivative CO_2 – in all the cases just mentioned, they were significant in the models as well. Further, and perhaps equally notably, each was shown to be Granger-causal to its relevant climate outcome.

A driver of the research for this paper has been the substantial pre-existing body of knowledge suggesting that the land biosphere is linked to the interannual (first-derivative) CO_2 signature. The new phenomenology characterised in this paper is consistent with the first-derivative results and adds the further phenomenology of the autocorrelation results. If plants are the agents of these phenomena it is required that plants contain mechanisms to: (i) detect rate of change of relevant environmental cues, including CO_2; and (ii) provide a capacity for "memory", for periods not only of months but years.

This section reviews evidence from plant research relevant to both these points.

We consider first the mechanism of plant responsiveness to atmospheric CO_2. Concerning responsiveness in general (for review see Volkov and Markin, 2012) it has been shown that plants can sense mechanical, electrical and electromagnetic stimuli, gravity, temperature, direction of light, insect attack, chemicals and pollutants, pathogens, water balance, etc. Concerning responsiveness to CO_2, for the stomata of plants – the plant components which regulate gas exchange including CO_2 and oxygen at the plant surface – extensive research (for example, see Maser et al., 2003) has shown that a network of signal transduction mechanisms integrates water status, hormone responses, light, CO_2 and other environmental conditions to regulate stomatal movements in leaves for optimization of plant growth and survival under diverse conditions.

ACPD
14, 29101–29157, 2014

While we have not been able to find studies measuring such sensitivity to stimuli in rate of change and acceleration terms – that is, in terms of first- and second-derivatives – nonetheless such sensitivity is widely present in animal systems, for example, in the form of acceleration detectors for limb control (Vidal-Gadea et al., 2010). Indeed Spitzer and Sejnowski (1997) argue that rather than occurring rarely, such differentiation and other computational processes are present and potentially ubiquitous in living systems, including at the single-celled level where a variety of biological processes – concatenations of chemical amplifiers and switches – can perform computations such as exponentiation, differentiation, and integration.

Plants with the ability to detect the rate of change of resources – especially scarce resources – would have a clear selective advantage. First and second derivatives, for example, are each leading indicators of change in the availability of a given resource. Leading indicators of change in CO_2 would enable a plant's photosynthetic apparatus to be ready in advance to harvest CO_2 when, for seasonal or other reasons, increasing amounts of it become available. In this connection, it is noteworthy that second-derivative capacity would provide greater advance warning than first.

Has CO_2 ever been such a scarce resource? According to Ziska (2008) plants evolved at a time of high atmospheric carbon dioxide (4–5 times present values), but concentrations appear to have declined to relatively low values during the last 25–30 million years. Therefore, it has been argued that for the last ca. 20 million years, terrestrial plant evolution has been driven by the optimisation of the use of its scarce "staple food", CO_2.

In this connection, a review by Franks et al.(2013) points out that plants have been equipped with most, if not all, of the fundamental physiological characteristics governing net CO_2 assimilation rate (e.g. stomata, chloroplasts, leaves, roots, hydraulic systems) for at least 370 million years. Given that atmospheric CO_2 has fluctuated at least five- to ten-fold its current ambient concentration over the same period, it is possible, even likely, that a generalised long-term net CO_2 assimilation rate vs. atmospheric CO_2 relationship evolved early in the history of vascular plants.

ACPD
14, 29101–29157, 2014

Turning to memory capacity, what mechanism in plants might provide it? Studies of vernalization – the capacity of some plants to flower in the spring only after exposure to prolonged cold – show (Amasino, 2004) that some plants must not only have the capacity to *sense* cold exposure but also have a mechanism to *measure the duration* of cold exposure and then *store* that information. In some species this "memory" of vernalization can be maintained for up to 330 days (Lang, 1965).

With the foregoing points, the plant model seems worthy of further consideration. Many of the questions of mechanism seem ideal for laboratory experiments.

The Supplement related to this article is available online at doi:10.5194/acpd-14-29101-2014-supplement.

Acknowledgements. The authors thank John Gordon, Carolyn Dawson and Jerry Silvey for useful discussions and support.

References

Adams, J. M. and Piovesan, G.: Long series relationships between global interannual CO_2 increment and climate: evidence for stability and change in role of the tropical and boreal-temperate zones, Chemosphere, 59, 1595–1612, 2005.

Amasino, R.: Vernalization, competence, and the epigenetic memory of winter. Historical perspective essay, Plant Cell, 16, 2553–2559, 2004.

Attanasio, A.: Testing for linear Granger causality from natural/anthropogenic forcings to global temperature anomalies, Theor. Appl. Climatol., 110, 281–289, 2012.

Attanasio, A. and Triacca, U.: Detecting human influence on climate using neural networks based Granger causality, Theor. Appl. Climatol., 103, 103–107, 2011.

Banerjee, A., Dolado, J., Galbraith, J. W., and Hendry, D. F.: Co-Integration, Error-Correction, and the Econometric Analysis of Non-Stationary Data, Oxford University Press, Oxford, 1993.

ACPD

14, 29101–29157, 2014

Granger causality from the 1st/2nd derivatives of atmospheric CO_2

L. M. W. Leggett and D. A. Ball

Barichivich, J., Briffa, K. R., Myneni, R. B., Osborn, T. J., Melvin, T. M., Ciais, P., Piao, S., and Tucker, C.: Large-scale variations in the vegetation growing season and annual cycle of atmospheric CO_2 at high northern latitudes from 1950 to 2011, Glob. Change Biol.,19, 3167–3183, 2013.
Bacastow, R. B.: Modulation of atmospheric carbon dioxide by the southern oscillation, Nature, 261, 116–118, 1976.
Bellenger, H., Guilyardi, E., Leloup, J., Lengaigne, M., and Vialard, J.: ENSO representation in climate models: from CMIP3 to CMIP5, Clim. Dynam., 42, 1999–2018, 2014.
Canty, T., Mascioli, N. R., Smarte, M. D., and Salawitch, R. J.: An empirical model of global climate – Part 1: A critical evaluation of volcanic cooling, Atmos. Chem. Phys., 13, 3997–4031, doi:10.5194/acp-13-3997-2013, 2013.
Meehl, G. A., C. Covey, T. Delworth, M. Latif, B. McAvaney, J. F. B. Mitchell, R. J. Stouffer, and K. E. Taylor, 2007: The WCRP CMIP3 multi-model dataset: A new era in climate change research, Bull. Am. Meteorol. Soc., 88, 1383–1394, (CMIP3) Multi-Model Mean20c3m/sresa1, http://climexp.knmi.nl/selectfield_CO2, last access 10 June 2014.
Chen, X. and Tung, K.: Varying planetary heat sink led to global-warming slowdown and acceleration, Science, 345, doi:10.1126/science.1254937, 2014.
Cox, P. M., Pearson, D., Booth, B. B., Friedlingstein, P., Huntingford, C., Jones, C. D., and Luke, C. M.: Sensitivity of tropical carbon to climate change constrained by carbon dioxide variability, Nature, 494, 341–344, 2013.
Denman, K. L., Brasseur, G., Chidthaisong, G., Ciais, A., Cox, P. P. M., Dickinson, P. M., Hauglustaine, R. E., Heinze, D., Holland, C. E., Jacob, D., Lohmann, U., Ramachandran, S., da Silva Dias, P. L., Wofsy, S. C., and Zhang, X.: Couplings between changes in the climate system and biogeochemistry, in: Climate Change 2007: The Physical Science Basis. Contribution of Working Group I to the Fourth Assessment Report of the Intergovernmental Panel on Climate Change, edited by: Solomon, S., Qin, D., Manning, M., Chen, Z., Marquis, M., Averyt, K. B., Tignor, M., and Miller, H. L., Cambridge University Press, Cambridge, United Kingdom and New York, NY, USA, 2007.
Keeling, R.-F., Piper, S.-C., Bollenbacher, A.-F., and Walker, S.-J.: Carbon Dioxide Research Group, Scripps Institution of Oceanography (SIO), University of California, La Jolla, California USA 92093-0444, Feb 2009., http://cdiac.ornl.gov/ftp/trends/co2/maunaloa.co2, last access: 14 July 2014, 2009.
Troup, A. J.: The Southern Oscillation, Quat. J. Roy. Meteorol. Soc., 91, 490–506, 1965.

ACPD
14, 29101–29157, 2014

Granger causality from the 1st/2nd derivatives of atmospheric CO_2

L. M. W. Leggett and D. A. Ball

Dieleman, W. I. J., Vicca, S., Dijkstra, F. A., Hagedorn, F., Hovenden, M. J., Larsen, K. S., Morgan, J. A., Volder, A., Beier, C., Dukes, J. S., King, J., Leuzinger, S., Linder, S., Luo, Y., Oren, R., De Angelis, P., Tingey, D., Hoosbeek, M. R., and Janssens, I. A.: Simple additive effects are rare: a quantitative review of plant biomass and soil process responses to combined manipulations of CO_2 and temperature, Glob. Change Biol., 18, 2681–2693, 2012.

Folland C.K., Colman A.W., Smith D.M., Boucher O., Parker D.E., and Vernier J.P. : Folland, C. K. et al.: High predictive skill of global surface temperature a year ahead, Geophys. Res. Lett., 40, 761–767, 2013.

Foster, G. and Rahmstorf, S.: Global temperature evolution 1979–2010, Environ. Res. Lett., 6, 044022, 2011.

Franks P.J., Adams M.A., Amthor J.S., Barbour M.M., Berry J.A., Ellsworth D.S., Farquhar G.D., Ghannoum O., Lloyd J., McDowell N., Norby R. J., Tissue D. T., and von Caemmerer S.: Sensitivity of plants to changing atmospheric CO_2 concentration: from the geological past to the next century, New Phytol., 197, 1077–1094, 2013.

Frisia, S., Borsato, A., Preto, N., and McDermott, F.: Late Holocene annual growth in three Alpine stalagmites records the influence of solar activity and the North Atlantic Oscillation on winter climate, Earth Planet. Sc. Lett., 216, 411–424, 2003.

Fyfe, J. C. and Gillett, N. P.: Recent observed and simulated warming, Nature Climate Change, 4, 150–151, 2014.

Fyfe, J. C., Gillett, N. P., and Zwiers, F. W.: Overestimated global warming over the past 20 years, Nature Climate Change, 3, 767–769, 2013.

Tucker, C. J., Pinzon, J. E., Brown, M. E., Slayback, D., Pak, E. W., Mahoney, R., Vermote, E., and El Saleous, N.: An extended AVHRR 8-km NDVI data set compatible with MODIS and SPOT vegetation NDVI data, Int. J. Remote Sens., 26, 4485–5598, 2005.

Granger, C. W. J.: Investigating causal relations by econometric models and cross-spectral methods, Econometrica, 37, 424–438, 1969.

Greene, W. H.: Econometric Analysis, 7th edn., Prentice Hall, Boston, 2012.

Gribbons, B. and Herman, J.: True and Quasi-Experimental Designs. Practical Assessment, Research and Evaluation, vol. 5, available at: http://PAREonline.net/getvn.asp?v=5&n=14, 1997.

Guemas, V., Doblas-Reyes, F. J., Andreu-Burillo, I., and Asif, M.: Retrospective prediction of the global warming slowdown in the past decade, Nature Climate Change, 3, 649–653, 2013.

Guilyardi, E., Bellenger H., Collins M., Ferrett S., Cai, W., and Wittenberg A.: A first look at ENSO in CMIP5, Clivar. Exch., 17, 29–32, 2012.
Ghosh, S. and Rao, C. R. (Eds.): Design and Analysis of Experiments, Handbook of Statistics, North-Holland, 13, 1996.
Hansen, J., Kharecha, P., and Sato, M.: Climate forcing growth rates: doubling down on our Faustian bargain, Environ. Res. Lett., 8, 2013.
Morice, C. P., Kennedy, J. J., Rayner, N. A., and Jones, P. D.: Quantifying uncertainties in global and regional temperature change using an ensemble of observational estimates: the HadCRUT4 dataset, J. Geophys. Res., 117, D08101, doi:10.1029/2011JD017187, 2012.
Hazewinkel, M. (Ed.): Finite-Difference Calculus, Encyclopedia of Mathematics, Springer, 2001.
Hidalgo, F. and Sekhon, J.: Causality, in: International Encyclopedia of Political Science, edited by: Badie, B., Berg-Schlosser, D., and Morlino, L., 204–211, 2011.
Holbrook, N. J., Davidson, J., Feng, M., Hobday, A. J., Lough, J. M., McGregor, S., and Risbey, J. S.: El Niño–Southern Oscillation, in: A Marine Climate Change Impacts and Adaptation Report Card for Australia 2009, edited by: Poloczanska, E. S., Hobday, A. J., and Richardson, A. J., NCCARF Publication, 2009.
Hume, D.: An Enquiry Into Human Understanding, 1751.
Hyndman, R. J.: Moving averages, in: International Encyclopedia of Statistical Science, edited by: Lovirc, M., Springer, New York, 866–869, 2010.
Imbers, J., Lopez, A., Huntingford, C., and Allen M. R.: Testing the robustness of the anthropogenic climate change detection statements using different empirical models, J. Geophys. Res.-Atmos., 118, 3192–3199, 2013.
IPCC: Climate Change 2007: The Physical Science Basis. Contribution of Working Group I to the Fourth Assessment Report of the Intergovernmental Panel on Climate Change, edited by: Qin, D., Manning, M., Chen, Z., Marquis, M., Averyt, K. B., Tignor, M., and Miller, H. L., Cambridge University Press, Cambridge, UK and New York, NY, USA, 2007.
IPCC: Climate Change 2013: The Physical Science Basis. Contribution of Working Group I to the Fifth Assessment Report of the Intergovernmental Panel on Climate Change, edited by: Stocker, T. F., Qin, D., Plattner, G.-K., Tignor, M., Allen, S. K., Boschung, J., Nauels, A., Xia, Y., Bex, V., and Midgley, P. M., Cambridge University Press, Cambridge, UK and New York, NY, USA, 1535 pp., 2013.

ACPD
14, 29101–29157, 2014

Katz, R. W.: Sir Gilbert Walker and a connection between El Niño and statistics, Stat. Sci., 17, 97–112, 2002.

Kaufmann, R. K., Kauppi, H., and Stock, J. H.: Emissions, concentrations, and temperature: a time series analysis, Climatic Change, 77, 249–278, 2006.

Kiviet, J. F.: On the rigour of some misspecification tests for modelling dynamic relationships, Rev. Econ. Stud., 53, 241–261, 1986.

Kodra, E., Chatterjee, S., and Ganguly, A. R.: Exploring Granger causality between global average observed time series of carbon dioxide and temperature, Theor. Appl. Climatol., 104, 325–335, 2011.

Kopp, G. and Lean, J. L.: A new, lower value of total solar irradiance: evidence and climate significance, Geophys. Res. Lett., 38, 2011.

Körner, C.: Plant CO_2 responses: an issue of definition, time and resource supply, New Phytol., 172, 393–411, 2006.

Kosaka, Y. and Shang-Ping, X.: Recent global-warming hiatus tied to equatorial Pacific surface cooling, Nature, doi:10.1038/nature12534, 2013.

Kuo, C., Lindberg, C., and Thomson, D. J.: Coherence established between atmospheric carbon dioxide and global temperature, Nature, 343, 709–714, 1990.

Lang, A.: A physiology of flower initiation, in: Encyclopedia of Plant Physiology, edited by: Ruhland, W., Springer-Verlag, Berlin, 1965.

Le Quéré, C., Peters, G. P., Andres, R. J., Andrew, R. M., Boden, T. A., Ciais, P., Friedlingstein, P., Houghton, R. A., Marland, G., Moriarty, R., Sitch, S., Tans, P., Arneth, A., Arvanitis, A., Bakker, D. C. E., Bopp, L., Canadell, J. G., Chini, L. P., Doney, S. C., Harper, A., Harris, I., House, J. I., Jain, A. K., Jones, S. D., Kato, E., Keeling, R. F., Klein Goldewijk, K., Körtzinger, A., Koven, C., Lefèvre, N., Maignan, F., Omar, A., Ono, T., Park, G.-H., Pfeil, B., Poulter, B., Raupach, M. R., Regnier, P., Rödenbeck, C., Saito, S., Schwinger, J., Segschneider, J., Stocker, B. D., Takahashi, T., Tilbrook, B., van Heuven, S., Viovy, N., Wanninkhof, R., Wiltshire, A., and Zaehle, S.: Global carbon budget 2013, Earth Syst. Sci. Data, 6, 235–263, doi:10.5194/essd-6-235-2014, 2014.

Lean, J. L. and Rind, D. H.: How natural and anthropogenic influences alter global and regional surface temperatures: 1889 to 2006, Geophys. Res. Lett., 35, 2008.

Lean, J. L. and Rind, D. H.: How will Earth's surface temperature change in future decades?, Geophys. Res. Lett., 36, L15708, 2009.

Lockwood, M.: Recent changes in solar outputs and the global mean surface temperature. III. Analysis of contributions to global mean air surface temperature rise, P. Roy. Soc. A-Math. Phy., 464, 1387–1404, 2008.

Maser, P., Leonhardt, N., and Schroeder, J. I.: The clickable guard cell: electronically linked model of guard cell signal transduction pathways, in: The Arabidopsis Book, available at: http://www-biology.ucsd.edu/labs/schroeder/clickablegc.html, 2003.

Meehl, G. A., Arblaster, J. M., Fasullo, J. T., Hu, A., and Trenberth, K. E.: Model-based evidence of deep-ocean heat uptake during surface-temperature hiatus periods, Nature Climate Change, doi:10.1038/NCLIMATE1229, 2011.

Moberg, A., Sonechkin, D. M., Holmgren, K., Datsenko, N. M., and Karlén, W.: Highly variable Northern Hemisphere temperatures reconstructed from low- and high-resolution proxy data, Nature, 433, 613–617, 2005.

Robertson, A., Overpeck, J., Rind, D., Mosley-Thompson, D. E., Zielinski, G., Lean, J., Koch, D., Penner, J., Tegen, I., and Healy, R.: Hypothesized climate forcing time series for the last 500 years, J. Geophys. Res., 106, 2001.

Running, S. W., Nemani, R. R., Heinsch, F. A., Zhao, M., Reeves, M. C., and Hashimoto, H.: A continuous satellite-derived measure of global terrestrial primary production, BioScience, 54, 547–560, 2004.

Sato, M., Hansen, J. E., McCormick, M. P., and Pollack, J. B. Stratospheric aerosol optical depths, 1850–1990, J. Geophys. Res., 98, 22987–22994, 1993.

Spitzer, N. C. and Sejnowski, T. J.: Biological information processing: bits of progress, Science, 277, 1060–1061, 1997.

Stahle, D. W., D'Arrigo, R. D., Krusic, P. J., Cleaveland, M. K., Cook, E. R., Allan, R. J., Cole, J. E., Dunbar, R. B., Therrell, M. D., Gay, D. A., Moore, M. D., Stokes, M. A., Burns, B. T., Villanueva-Diaz, J., and Thompson, L. G.: Experimental dendroclimatic reconstruction of the Southern Oscillation, B. Am. Meteorol. Soc., 79, 2137–2152, 1998.

Steger, U., Achterberg, W., Blok, K., Bode, H., Frenz, W., Gather, C., Hanekamp, G., Imboden, D., Jahnke, M., Kost, M., Kurz, R., Nutzinger, H. G., and Ziesemer, T.: Sustainable Development and Innovation in the Energy Sector, Springer, Berlin, 2005.

Stern, D. I. and Kander, A.: The Role of Energy in the Industrial Revolution and Modern Economic Growth, CAMA Working Paper Series, Australian National University, 2011.

Stern, D. I. and Kaufmann, R. K.: Anthropogenic and natural causes of climate change, Climatic Change, 122, 257–269, doi:10.1007/s10584-013-1007-x, 2014.

Sun, L. and Wang, M.: Global warming and global dioxide emission: an empirical study, J. Environ. Manage., 46, 327–343, 1996.
Toda, H. Y. and Yamamoto, T.: Statistical inferences in vector autoregressions with possibly integrated processes, J. Econometrics, 66, 225–250, 1995.
Troup, A. J.: The southern oscillation, Q. J. Roy. Meteor. Soc., 91, 490–506, 1965.
Triacca, U.: Is Granger causality analysis appropriate to investigate the relationship between atmospheric concentration of carbon dioxide and global surface air temperature?, Theor. Appl. Climatol., 81, 133–135, 2005.
Tung, K.-K. and Zhou, J.: Using data to attribute episodes of warming and cooling in instrumental records, P. Natl. Acad. Sci. USA, 110, 2058–2063, 2013.
Vidal-Gadea, A. G., Jing, X. J., Simpson, D., Dewhirst, O., Kondoh, Y., and Allen, R.: Coding characteristics of spiking local interneurons during imposed limb movements in the locust, J. Neurophysiol., 103, 603–615, 2010.
Volkov, A. G. and Markin, V. S.: Phytosensors and phytoactuators, in: Plant Electrophysiology Signaling and Responses, edited by: Volkov, A. G., Springer-Verlag, Berlin, 369 pp., 2012.
Wang, C., Deser, C., Yu, J.-Y., DiNezio, P., and Clement, A.: El Niño-Southern Oscillation (ENSO): a review, in: Coral Reefs of the Eastern Pacific, Glynn, P. Manzello, D., and Enochs, I., Springer Science, 2012.
Wang, W., Ciais, P., Nemani, R. R., Canadell, J. G., Piao, S., Sitch, S., White, M. A., Hashimoto, H., Milesi, C., and Myneni, R. B.: Variations in atmospheric CO_2 growth rates coupled with tropical temperature, Proc. Natl. Acad. Sci. USA, 110, 13061–13066, 2013.
Zhang, Y., Guanter, L., Berry, J. A., Joiner, J., van der Tol, C., Huete, A., Gitelson, A., Voigt. M., and Köhler, P.: Estimation of vegetation photosynthetic capacity from space-based measurements of chlorophyll fluorescence for terrestrial biosphere models, Glob. Change Biol., doi:10.1111/gcb.12664, 2014.
Zhou, J. and Tung, K.: Deducing multidecadal anthropogenic global warming trends using multiple regression analysis, J. Atmos. Sci., 70, 1–8, 2013.
Ziska, L. H.: Rising atmospheric carbon dioxide and plant biology: the overlooked paradigm, in: Controversies in Science and Technology, from Climate to Chromosomes, edited by: Kleinman, D. L., Cloud-Hansen, K. A. et al., Liebert Inc., New Rochele, 379–400, 2008.

Table 1. Lag of first-derivative CO_2 relative to surface temperature series for global, tropical, Northern Hemisphere and Southern Hemisphere categories.

	Lag in months of first-derivative CO_2 relative to global surface temperature category
hadcrut4SH	−1
hadcrut4Trop	−1
HadCRUT4_nh	−3
hadcrut4Glob	−2

ACPD
14, 29101–29157, 2014

Table 2. Lag of FIRST-DERIVATIVE CO_2 relative to surface temperature series for global, tropical, Northern Hemisphere and Southern Hemisphere categories, each for three time-series sub-periods.

Temperature category	Time period	Lag of first-derivative CO_2 relative to global surface temperature series
NH	1959.87–1976.46	−6
NH	1976.54–1993.21	−6
Global	1959.87–1976.46	−4
SH	1959.87–1976.46	−3
Global	1976.54–1993.21	−2
Tropical	1959.87–1976.46	0
Tropical	1976.54–1993.21	0
Tropical	1993.29–2012.37	0
Global	1993.29–2012.37	0
NH	1993.29–2012.37	0
SH	1976.54–1993.21	0
SH	1993.29–2012.37	0

ACPD
14, 29101–29157, 2014

L. M. W. Leggett and D. A. Ball

Table 3. Augmented Dickey–Fuller (ADF) test for stationarity for monthly data 1969 to 2012 for global surface temperature, level of atmospheric CO_2 and first-derivative CO_2.

	ADF statistic	p value	Test interpretation
TEMP	−6.942	0.000	Stationary
FIRST-DERIVATIVE CO_2	−4.646	0.001	Stationary
CO_2	−1.222	0.904	Non-stationary

ACPD
14, 29101–29157, 2014

Table 4. Pairwise correlations (correlation coefficients (R)) between selected climate variables.

	2x13mmafirstderivCO2	Hadcrut4Global	3x13mma2ndderivCO2
Hadcrut4Global	**0.7**	1	
3x13mma2ndderivCO2	0.06	−0.05	1
13mmaReverseSOI	0.25	0.14	**0.37**

ACPD
14, 29101–29157, 2014

Granger causality from the 1st/2nd derivatives of atmospheric CO_2

L. M. W. Leggett and D. A. Ball

Table 5. Pairwise correlations (correlation coefficients (R)) between selected climate variables, phase-shifted as shown in the table.

	Led2m2x13mmafirstderivCO2	Hadcrut4Global	Led4m3x13mma2ndderivCO2
Hadcrut4Global	**0.71**	1	
Led4m3x13mma2ndderivCO2	0.23	0.09	1
13mmaReverseSOI	0.16	0.14	**0.49**

Discussion Paper | Discussion Paper | Discussion Paper | Discussion Paper |
ACPD
14, 29101–29157, 2014

Table 6. Pairwise correlations (correlation coefficients (R)) between selected climate variables, phase-shifted as shown in the table.

	ZLed2m2x13mma2ndderivCO2	ZReversesignSOI
ZReversesignSOI	0.28	1.00
ZLed3m13mmafirstderivhadcrut4global	0.35	0.41

ACPD
14, 29101–29157, 2014

ACPD
14, 29101–29157, 2014

L. M. W. Leggett and D. A. Ball

Table 7. Augmented Dickey–Fuller (ADF) test for stationarity for monthly data 1959 to 2012 for second-derivative CO_2 and sign-reversed SOI.

	ADF statistic	p value	Test interpretation
Second-derivative CO_2	−10.077	0.000	Stationary
Sign-reversed SOI	−6.681	0.000	Stationary

Table 8. VAR Residual Serial Correlation LM Tests component of Granger-causality testing of relationship between second-derivative CO_2 and SOI. Initial 2-lag model

Lag order	LM-Stat	*P* value*
1	10.62829	0.0311
2	9.71675	0.0455
3	2.948737	0.5664
4	9.711391	0.0456
5	10.67019	0.0305
6	37.13915	0
7	1.268093	0.8668

* *P* values from chi-square with 4 df.

ACPD
14, 29101–29157, 2014

Table 9. VAR Residual Serial Correlation LM Tests component of Granger-causality testing of relationship between second-derivative CO_2 and SOI. Preferred 3-lag model

Lag order	LM-Stat	*P* value*
1	1.474929	0.8311
2	4.244414	0.3739
3	2.803332	0.5913
4	13.0369	0.0111
5	8.365221	0.0791
6	40.15417	0
7	1.698265	0.791

* *P* values from chi-square with 4 df.

ACPD
14, 29101–29157, 2014

Table 10. Correlations (R) between paleoclimate CO_2 and temperature estimates 1500–1940.

	Temperature (speliothem)	Temperature (tree ring)
Level of CO_2 (ice core)	0.369	0.623
1st deriv. CO_2 (ice core)	0.558	0.721

ACPD
14, 29101–29157, 2014

Table 11. Stationarity (Dickey–Fuller) test statistics for NDVI and climate variables.

	ADF statistic	P value	Test interpretation
NDVI	−5.40	7.82×10^{-5}	Stationary
Gap (CO_2 minus Had4Glob)	−4.26	3.79×10^{-3}	Stationary
SOI	−4.99	4.69×10^{-4}	Stationary

ACPD
14, 29101–29157, 2014

Table 12. Quantitative results summarised.

Independent variable	Dependent variable	Period studied	Frequency	Number of observations	Climate var regression coefficient	Climate var *P* value	Whole model adjusted *R*-squared	Whole model *p* value
Led2m2x13mma1stDerivCO2 Led1mHad4Glob Led2mHad4Glob	Had4Glob	1959–2012	Monthly	640	0.0973641	< 0.00001	0.861279	6.70E-273
Led3mZ2x13mma2ndDerivCO2 Led1mZReversesignSOI Led2mZReversesignSOI	ZReversesignSOI	1960–2012	Monthly	637	0.0769493	0.01059	0.477552	1.80E-89
led3mZ13mma_first_derivhad4Glob Led1mZReversesignSOI Led2mZReversesignSOI	ZReversesignSOI	1877–2012	Monthly	1629	0.140219	< 0.00001	0.465612	3.80E-221
1st deriv. CO_2 (ice core)	Temperature (speliothem)	1500–1940	Annual	440			0.311	n.a.
1st deriv. CO_2 (ice core)	Temperature (tree ring)	1627–1928	Annual	440			0.52	n.a.
Level of CO_2 (ice core)	Temperature (tree ring)	1627–1928	Annual	440			0.388	n.a.
led4mNDVI led1mGap (CO_2 minus Had4Global) led2mGap (CO_2 minus Had4Global)	Gap (CO_2 minus Had4Glob)	1981–2013	Monthly	376	0.0462155	0.09228	0.524683	2.09E-60
ZSOI Led 1mNDVI	NDVI	1981–2013	Monthly	374	0.12	0.00053	0.5273	1.59E-61

ACPD
14, 29101–29157, 2014

Discussion Paper | Discussion Paper | Discussion Paper | Discussion Paper |
Title Page
Abstract | Introduction
Conclusions | References
Tables | Figures
◄◄ | ►►
◄ | ►
Back | Close
Full Screen / Esc
Printer-friendly Version
Interactive Discussion

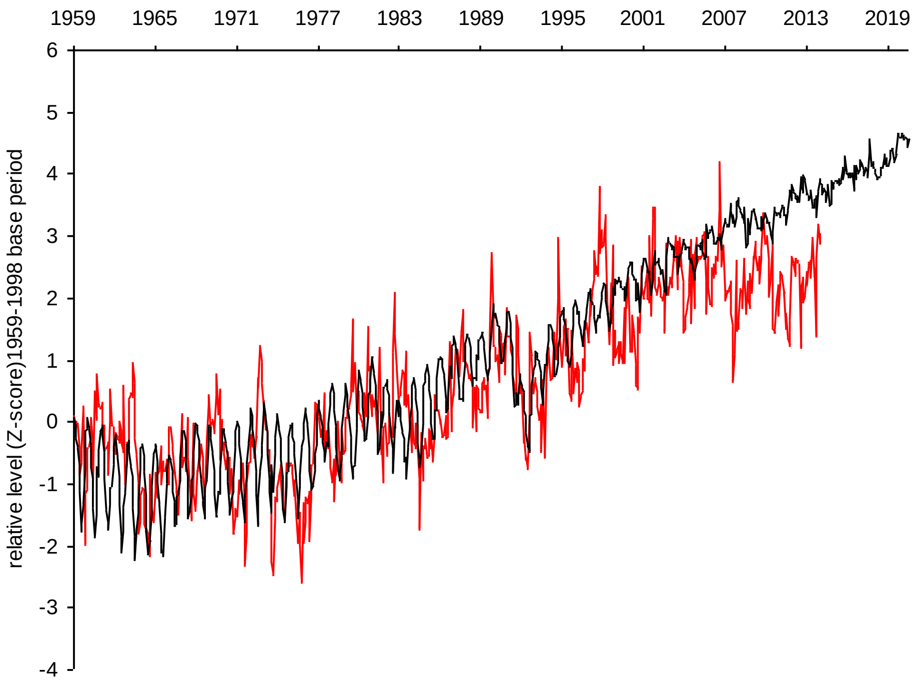

Figure 1. Monthly data: global surface temperature (HADCRUT4 dataset) (red curve) and an IPCC mid-range scenario model (CMIP3, SRESA1B scenario) run for the IPPC fourth assessment report (IPCC, 2007) (blue curve), each expressed in terms of Z scores to aid visual comparison (see Sect. 1).

ACPD
14, 29101–29157, 2014

Granger causality from the 1st/2nd derivatives of atmospheric CO_2

L. M. W. Leggett and D. A. Ball

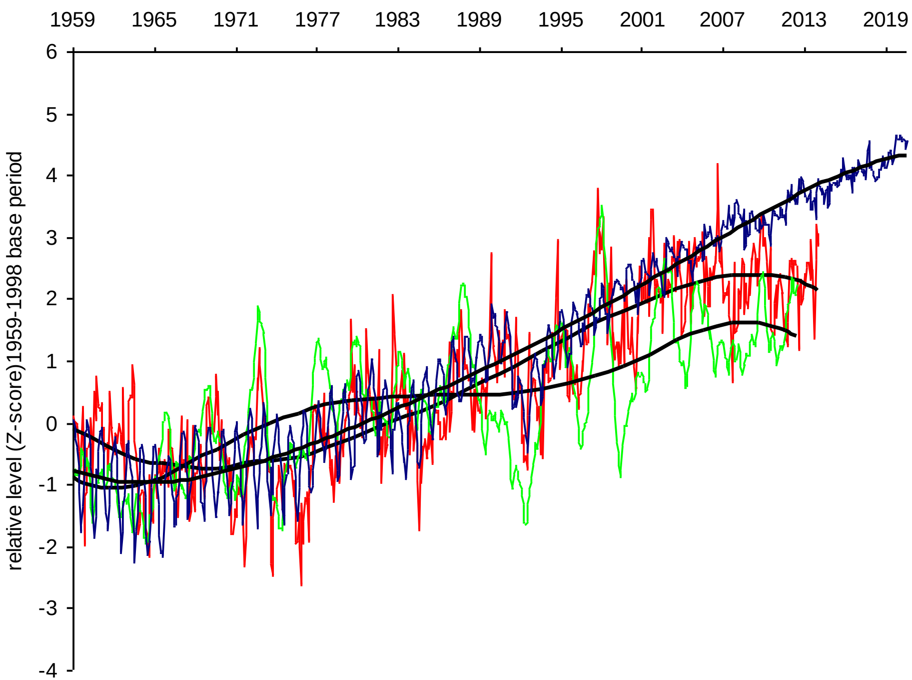

Figure 2. *Z* scored monthly data: global surface temperature (green curve) compared to an IPCC mid-range scenario model (CMIP3, SRESA1B scenario) run for the IPCC fourth assessment report (IPCC, 2007) (blue curve) and also showing the trend in first-derivative atmospheric CO_2 (smoothed by two 13 month moving averages) (red curve). To show their core trends for illustrative purposes the three series are fitted with 5th order polynomials.

ACPD
14, 29101–29157, 2014

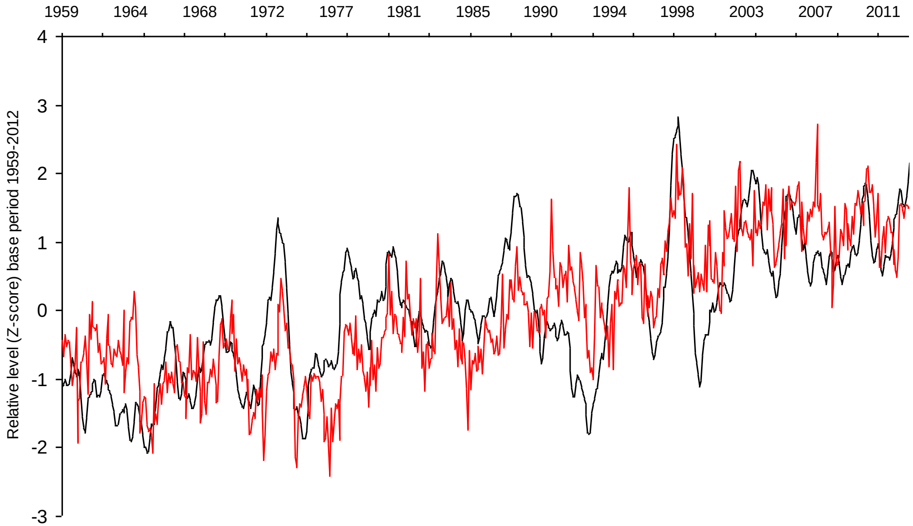

Figure 3. Z scored monthly data: global surface temperature (red curve) compared to first-derivative atmospheric CO_2 smoothed by two 13 month moving averages (black curve).

ACPD
14, 29101–29157, 2014

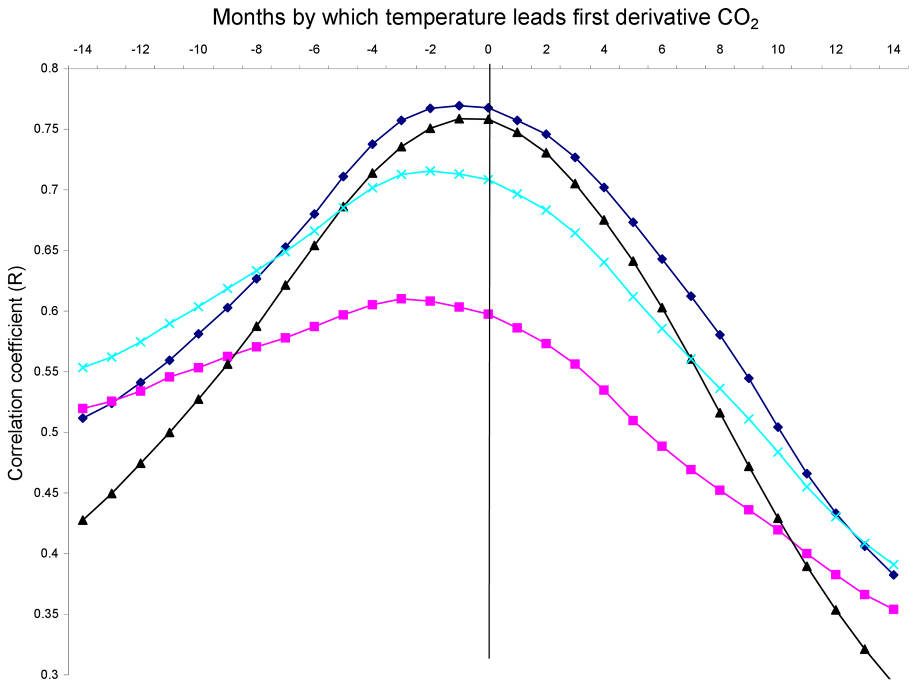

Figure 4. Correlograms of first-derivative CO_2 with surface temperature for global (turquoise curve), tropical (black), Northern Hemisphere (purple) and Southern Hemisphere (blue) categories.

ACPD

14, 29101–29157, 2014

Granger causality from the 1st/2nd derivatives of atmospheric CO_2

L. M. W. Leggett and D. A. Ball

Title Page
Abstract | Introduction
Conclusions | References
Tables | Figures
◀I | ▶I
◀ | ▶
Back | Close
Full Screen / Esc
Printer-friendly Version
Interactive Discussion

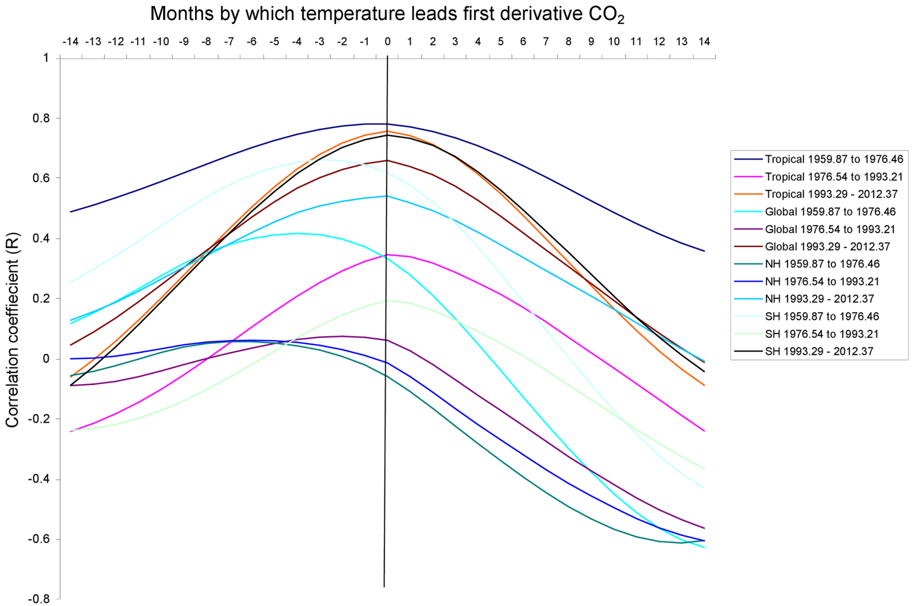

Figure 5. Correlograms of first-derivative CO_2 with surface temperature for global, tropical, Northern Hemisphere and Southern Hemisphere categories, each for three time-series sub-periods.

ACPD
14, 29101–29157, 2014

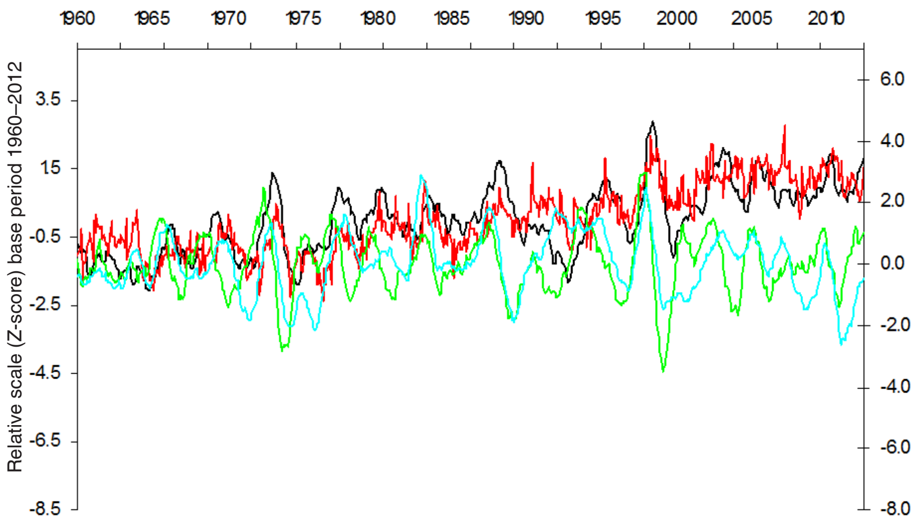

Figure 6. *Z* scored monthly data: global surface temperature (red) and first-derivative atmospheric CO_2 smoothed by two 13 month moving averages (black) (left-hand scale); and sign-reversed SOI smoothed by a 13 month moving average (blue) and second-derivative atmospheric CO_2 smoothed by three 13 month moving averages (green) (right-hand scale).

ACPD
14, 29101–29157, 2014

Granger causality from the 1st/2nd derivatives of atmospheric CO_2

L. M. W. Leggett and D. A. Ball

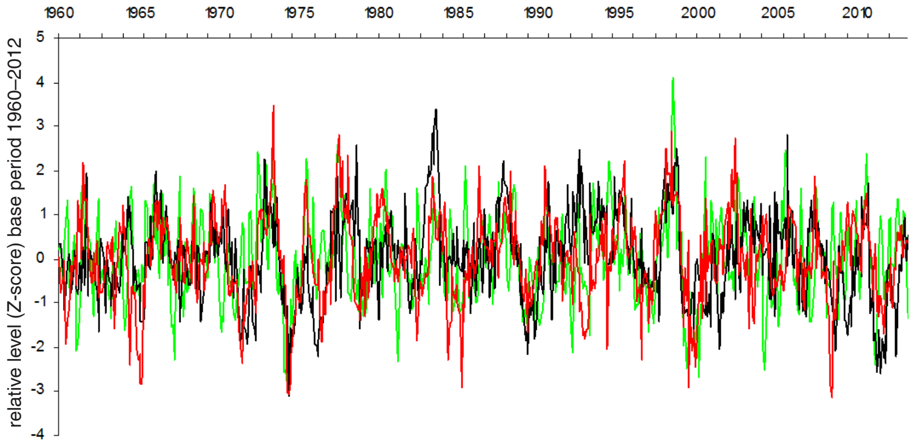

Figure 7. Z scored monthly data: sign-reversed SOI (unsmoothed and neither led nor lagged) (black); second-derivative CO_2 smoothed by a 13 month × 13 month moving average and led relative to SOI by 2 months (green); and first-derivative global surface temperature smoothed by a 13 month moving average and led by 3 months (red).

ACPD
14, 29101–29157, 2014

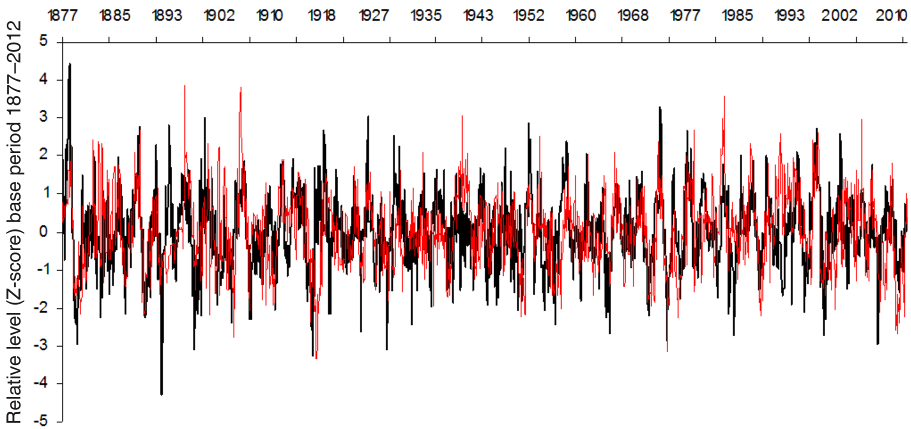

Figure 8. Z scored monthly data: sign-reversed SOI (unsmoothed and neither led nor lagged) (red); and first-derivative global surface temperature smoothed by a 13 month moving average and led relative to SOI by 3 months (green).

ACPD
14, 29101–29157, 2014

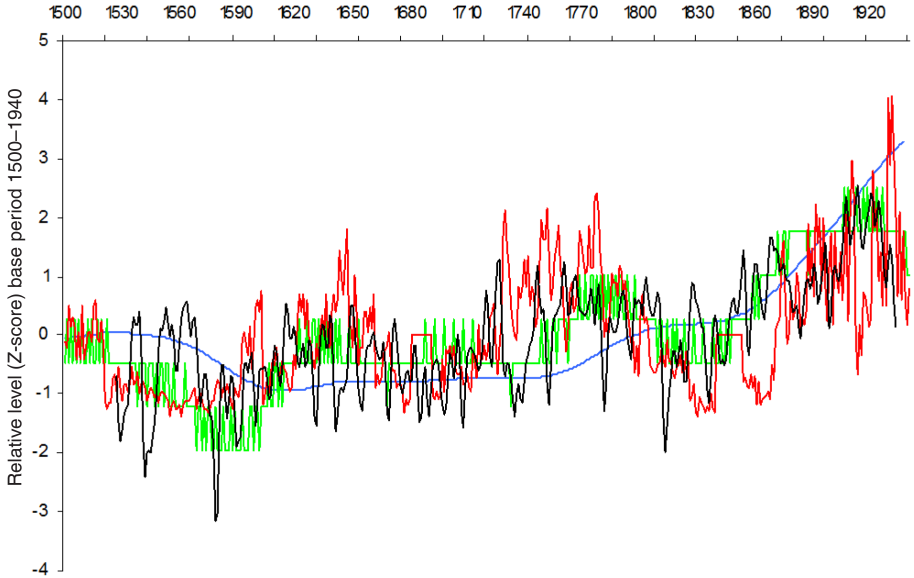

Figure 9. *Z* scored annual data: paleoclimate time series from 1500: ice core level of CO_2 (blue), level of CO_2 transformed into first derivative form (green); and temperature from speliothem (red) and tree ring data (black).

ACPD
14, 29101–29157, 2014

Granger causality from the 1st/2nd derivatives of atmospheric CO_2

L. M. W. Leggett and D. A. Ball

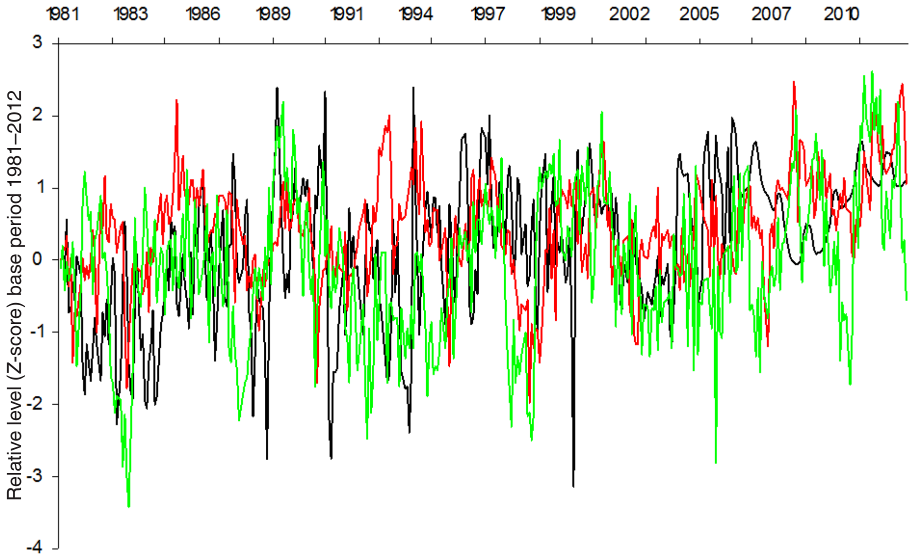

Figure 10. Z scored monthly data: observed trends in: the difference between the observed level of atmospheric CO_2 and global surface temperature (red); the Southern Oscillation Index (green); and global NDVI (black).